PNAS

Supporting Information for

HDX-MS finds that partial unfolding with sequential domain activation controls condensation of a cellular stress marker

Ruofan Chen[1], Hendrik Glauninger[2,3], Darren N. Kahan[2], Julia Shangguan[2], Joseph R. Sachleben[4], Joshua A. Riback[2,3,†], D. Allan Drummond[2], Tobin R. Sosnick[1,2,5*]

Tobin R. Sosnick
Email: trsosnic@uchicago.edu

This PDF file includes:

Supporting text
Figure S1 to S13
Table S1
SI References

Supporting Information Text

HDX formalism. In the Linderstrom-Lang model for HDX (1), the protein backbone amide proton is exchange-incompetent when it forms a protein-protein H-bond (closed state). The H-bond can be broken upon a conformational change and become available for exchange (open state):

$$H_{closed} \underset{k_{close}}{\overset{k_{open}}{\rightleftharpoons}} H_{open} \xrightarrow{k_{chem}} D$$

where k_{chem} is the intrinsic rate of exchange in the open state for an exposed amide proton, and k_{open} and k_{close} are the rates of opening and closing in the transition from the closed (H_{closed}) to open state (H_{open}), respectively. The steady-state solution is:

$$k_{obs} = \frac{k_{open} k_{chem}}{k_{open} + k_{close} + k_{chem}}$$

Depending on the relative rates, HDX falls into two different regimes yielding different information. When $k_{close} \ll k_{chem}$, $k_{obs} \sim k_{open}$. In this "EX1" regime, the observed rate is governed just by the opening rate. When $k_{close} \gg k_{chem}$, $k_{obs} = k_{chem} * k_{open}/k_{close} = k_{chem}/K_{eq}$ where $K_{eq} = k_{closed}/k_{open}$ is the equilibrium constant between the open and closed states. In this "EX2" regime, the observed rate is determined by K_{eq} in combination with k_{chem}.

In EX2 regime, the ratio between k_{chem} and k_{obs}, which is termed protection factor (*PF*), yields the information of structural stability according to the relationship between gibbs free energy and reaction constant.

$$\text{Protection factor } (PF) = k_{chem}/k_{obs} = K_{eq} + 1$$

$$\Delta G = -RT \ln K_{eq}$$

One can either analyze HDX data at the peptide level or resolve the uptake of each residue by subtracting overlapping peptides, which is a trade-off between resolution and accuracy. Here, we analyze HDX at the peptide level. The uptake of a peptide is a sum of uptakes from each residue and the calculated protection factor reflects the average stability of the peptide region across each residue.

There are different ways to distinguish EX1 and EX2 regimes, including their different pH dependences. The observed rate, k_{obs}, in the EX2 regime will change according to the change in the intrinsic rate, k_{chem}, but will not for the EX1 regime (assuming K_{eq} and k_{open} are pH insensitive).

In addition, EX1 and EX2 regimes result in different isotopic distribution behavior on mass spectra. In the EX2 regime where multiple opening events occur before a given amide proton is likely to exchange, the mass envelope shifts continuously to higher MW with an isotope distribution that satisfies the binomial distribution reflecting the stochasticity and independent exchange behavior of each amide protein (and other natural isotopes). For ideal EX1 exchange kinetics, however, there is the concerted exchange of multiple amides in an opening event that results in the decrease of one peak and a commensurate increase in another peak centered at an MW that is higher by the number of exchanged sites. One can have mixed behavior with some sites exchanging with EX2 kinetics and others with EX1 kinetics. Generally, each peak maintains its amplitude while it continuously shifts to higher MW reflecting the EX2 kinetics while a more drastic shift in populations from one peak to the other can occur reflecting EX1 kinetics.

Supplementary Figures

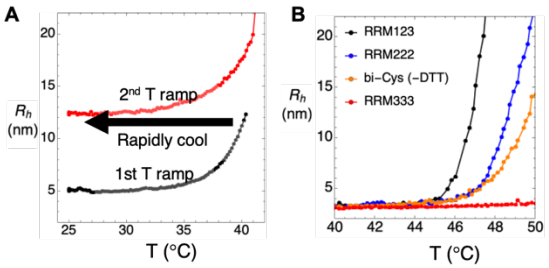

Fig. S1. (A) Pab1 condensation is irreversible by cooling and pre-formed condensates do not nucleate condensation at temperatures below T_{cond}. Sample was heated to the onset of condensation (at 40 °C, 1 °C above T_{cond} = 39 °C) and then cooled back to 25 °C for 20 min. The R_h level, 11.5 nm, did not change during cooling. The sample was then reheated and the same temperature-dependent profile in R_h as observed in the initial heat ramp. **(B)** Bi-Cys mutant under oxidizing condition has nearly the same T_{cond} as RRM222.

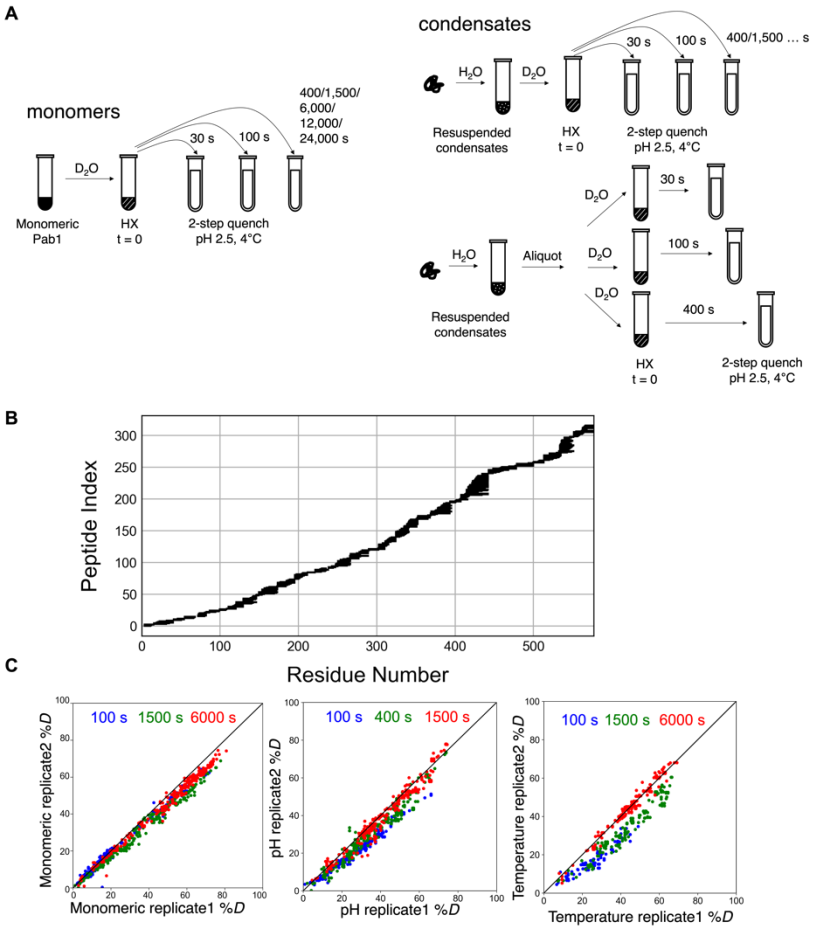

Fig. S2. Pab1 HDX protocol and reproducibility of data. (A) Labeling protocols for monomeric Pab1 and condensates. The samples at each time point were taken either from a single bulk exchanging sample, or from individual samples exchanging separately. The two protocols produced consistent results as shown in (C). **(B)** Pab1 HDX-MS peptides coverage map**. (C)** Comparison of *D%* for two replicates for monomeric Pab1, and temperature- and pH-condensates.

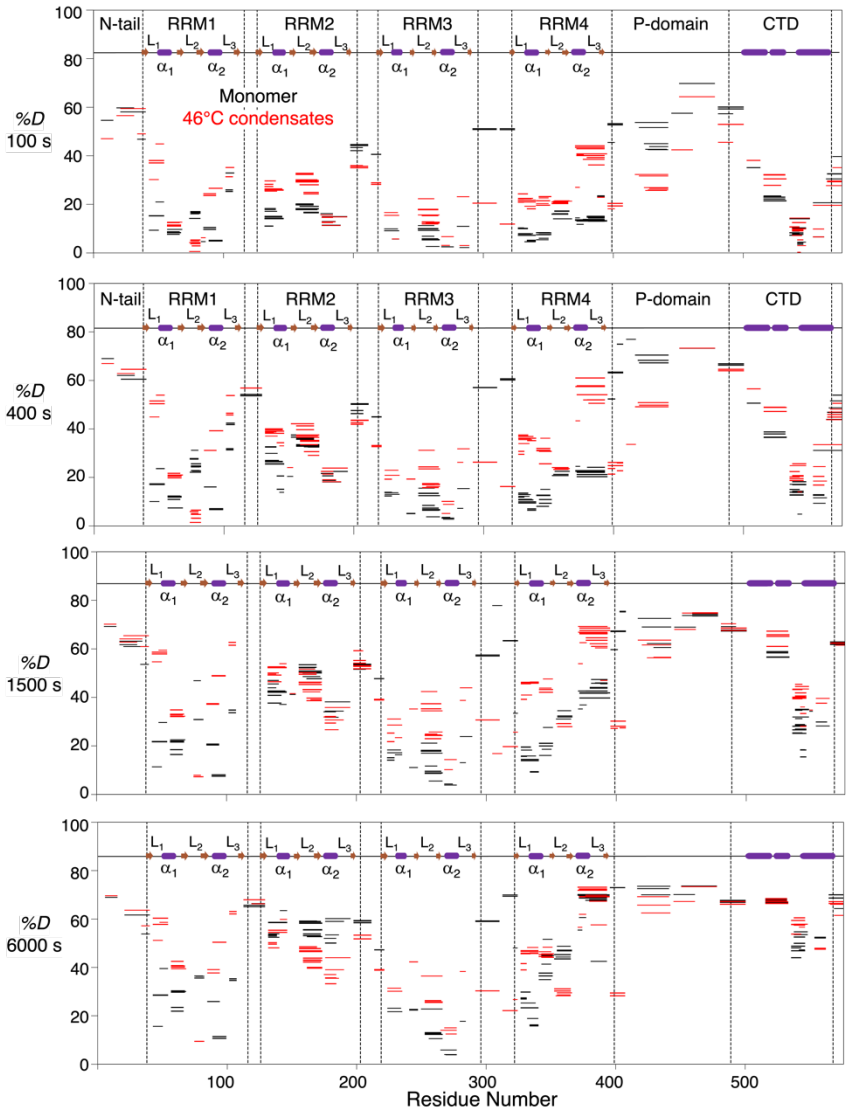

Fig. S3. Wood's plots comparing %D uptake of the soluble and 46 °C-induced condensed states at t_{HDX} = 100 s, 400, 1500 and 6,000 s.

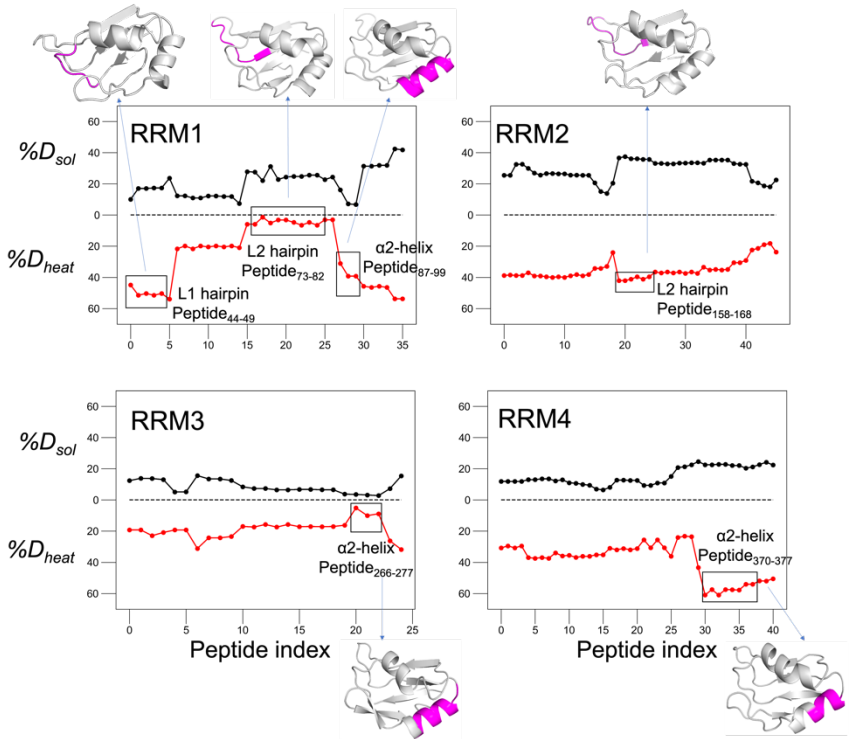

Fig. S4. Butterfly plots comparing *%D* of monomers and temperature-induced condensates at t_{HDX} = 400 s. Each point represents a peptide in the direction from N-termini to C-termini. Regions exhibiting the most significant differences between the two states are highlighted.

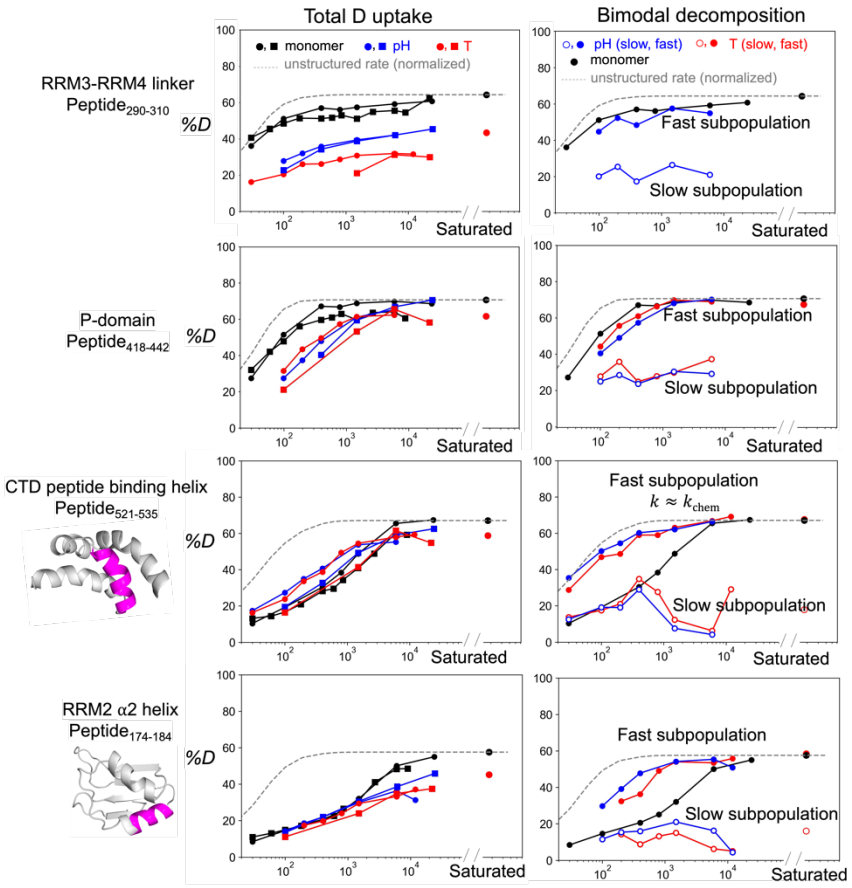

Fig. S5. D uptake curves for the RRM3-RRM4 linker, P-domain, CTD, and α2 helix in RRM2. Left: Total *%D* uptake curve for the combined fast and slow subpopulations from 2 replicates. Right: *%D* uptake curves for the fast and the slow subpopulations obtained using a bimodal fitting procedure. One replicate is shown for clarity. HDX of Peptide$_{418\text{-}442}$ from the P-domain displayed heterogeneity with a slow subpopulation (see Fig. 2B-C). The C-terminal domain (CTD) Helix 2 (Peptide$_{521\text{-}535}$, part of the CTD's peptide binding site (2), was unfolded for the majority of the molecules (see Fig. 2B-C), which potentially led to a disruption of the hydrophobic core and destabilization of other regions of the CTD). The non-monotonic behavior in the uptake curves for the slow population in the middle and bottom right panels could be due to artifacts in the bimodal fitting or the presence of a third population.

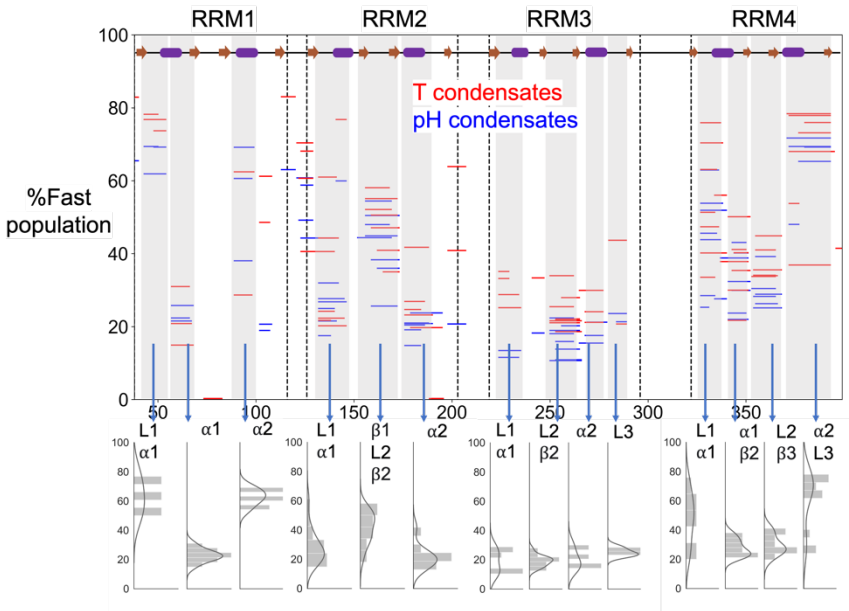

Fig. S6. Heterogeneity map of Pab1 condensates induced by temperature (46 °C) or pH. Fractions of the faster-exchanging subpopulation for RRM regions that become unfolded in the condensates are plotted against the sequence. Peptides from the structured regions are shown. Density distributions of %Faster population for peptides from each secondary structure (depicted on top, rectangles for helices, arrows for strands) are shown at the bottom of the plot.

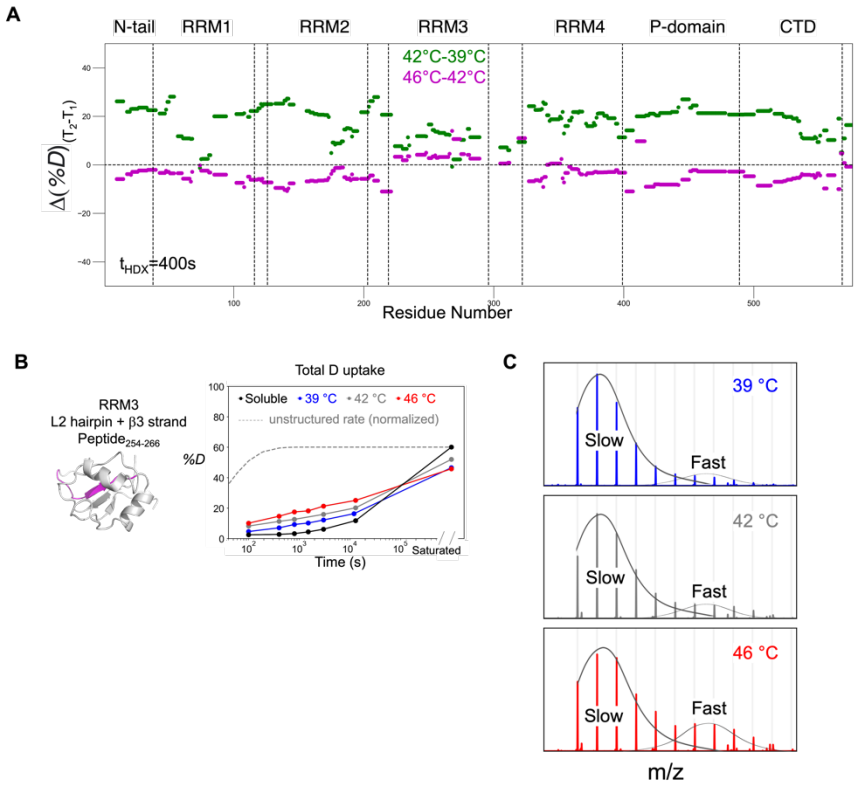

Fig. S7. Temperature-dependent HDX profiles RRM3. Because Pab1 condensation can be triggered at temperatures as low as 37°C, albeit with slower kinetics (3), we were able to create samples of Pab1 condensates at 39°C (overnight), 42°C (3 hours), and 46°C (20 min) at pH 6.5.The increased condensation times at 39 and 42° C, and at reduced pH (pH 6.8 for the 46 °C condensate mentioned in the HDX data presented elsewhere in this paper) were needed to generate sufficient material for HDX analysis. **(A)** Comparing the D uptake of condensates between 39 and 42°C (green) and between 42 and 46°C (purple) at t_{HDX}=400s. The D uptake for each residue is calculated as the average of uptakes from all peptides covering the residue. **(B)** Uptake curve for RRM3 $Pep_{254-266}$ and **(C)** corresponding mass spectra at t_{HDX} = 3,000 s for condensates formed at 3 different temperatures.

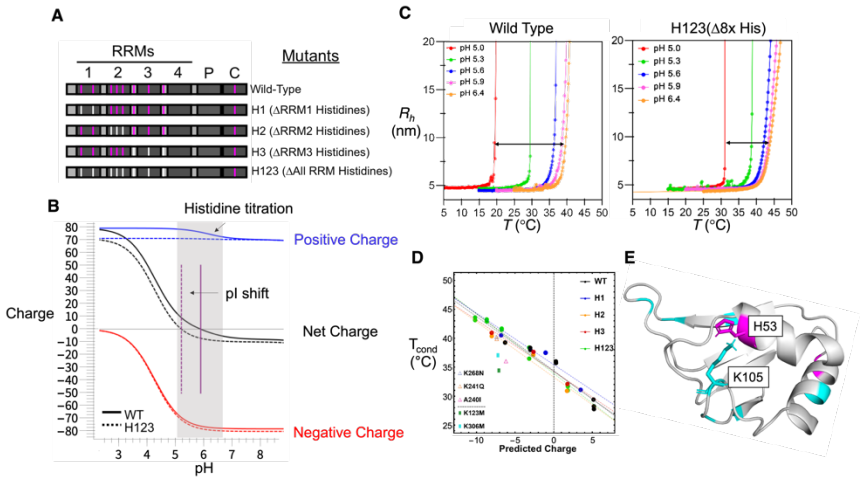

Fig. S8. pH response and histidines. (A) Histidine mutants where histidines from each or all RRMs are substituted with the next most common amino acid (3). **(B)** Titration curve of WT Pab1 and H123 mutant. Histidine titration overlaps with Pab1's condensing pH. **(C)** T_{cond} of H123 decreased by 12 °C when pH was reduced from 6.4 to 5.0, whereas WT Pab1 experienced a 20 °C decrease. This decrease in pH sensitivity implies that histidines are partly responsible for Pab1's response to acidification. **(D)** Predicted charges of Pab1's histidine mutants correlate with their T_{cond} at different pHs. A previous phase separation study investigated a broader range of net charge and observed that the saturation concentration (c_{sat}) was the lowest around charge neutrality (4). Some non-histidine mutants deviate from the line indicating Pab1's different sensitivities to these mutations. **(E)** Histidines (magenta) and other positively charged residues (cyan) on RRM1. Specifically, the positive charges on H53 and K105 are estimated to be 3.9 Å apart. Upon acidification and histidine protonation, the Coulombic repulsion may cause local unfolding and subsequent condensation. Nevertheless, the titration of histidine does not fully explain Pab1's pH response as some regions without histidines were similarly destabilized/unfolded upon pH-induced condensation.

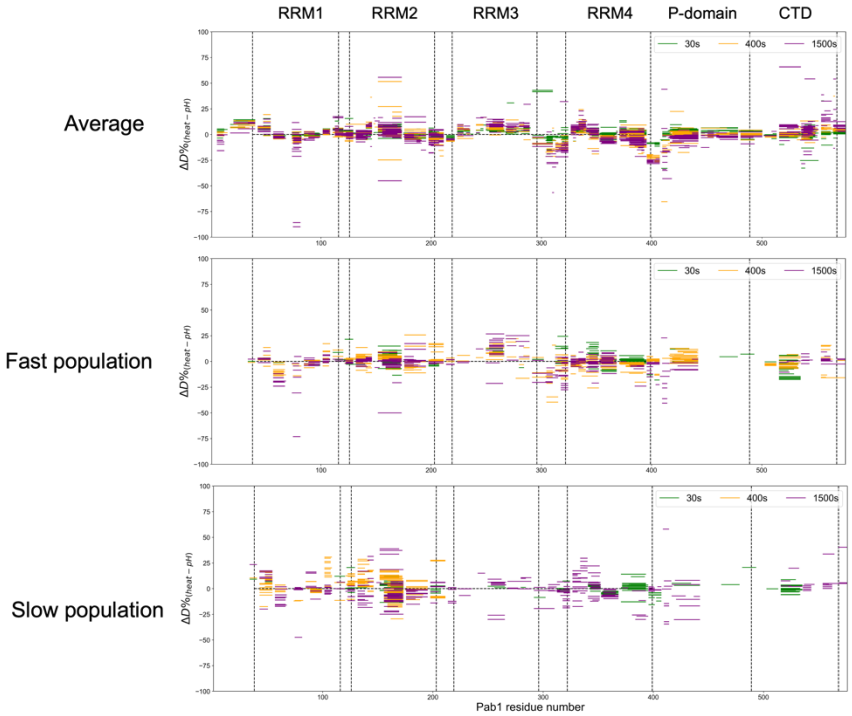

Fig. S9. *%D* difference between temperature- and pH-induced condensates at 3 exchange times. Upper: *%D* difference of the total uptake (combining the fast and slow subpopulations for regions with heterogeneity). Middle: *%D* difference of the faster exchanging subpopulation. Lower: *%D* difference of the slower exchanging subpopulation.

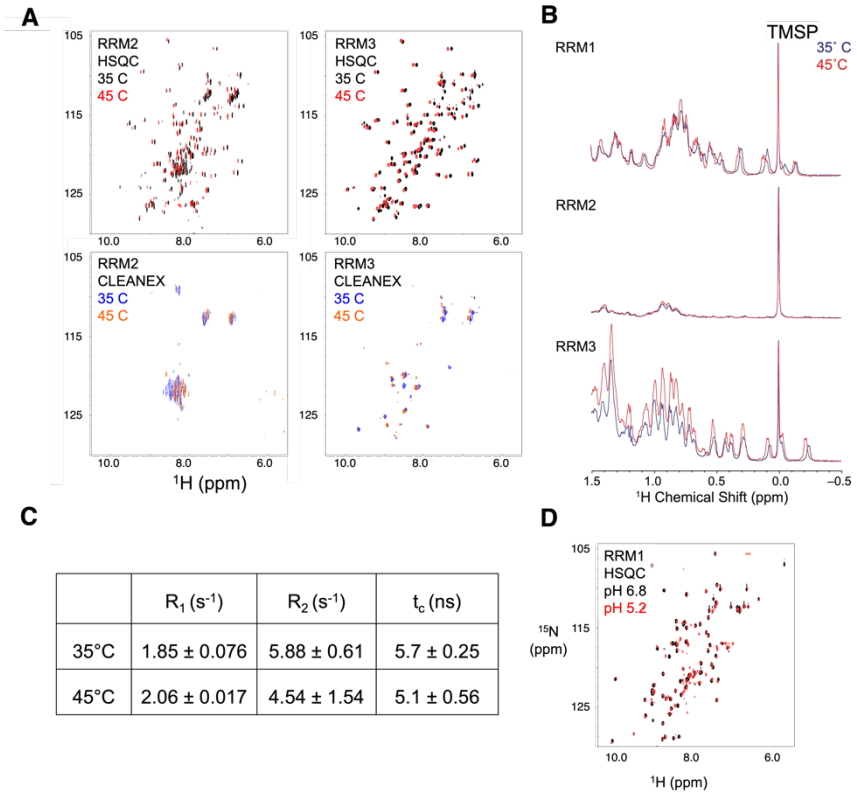

	R_1 (s^{-1})	R_2 (s^{-1})	t_c (ns)
35°C	1.85 ± 0.076	5.88 ± 0.61	5.7 ± 0.25
45°C	2.06 ± 0.017	4.54 ± 1.54	5.1 ± 0.56

Fig. S10. NMR indicates that individual RRMs remain well-folded above Pab1 T_{cond} or below Pab1 pH_{cond}. (A) $^1H^{15}N$ NMR HSQC spectra (upper) of RRM2 and 3, at 35 and 45°C, pH 6.8, and corresponding water saturation transfer (CLEANEX (5)) spectra (lower) at the same conditions. **(B)** Overlaid ^1H spectrum at 35 and 45°C comparing methyl peaks and the reference compound. **(C)** Relaxation measurements of RRM1. **(D)** Overlaid $^1H^{15}N$ NMR HSQC spectrum of RRM1 at pH 6.8 and pH 5.2, 30°C.

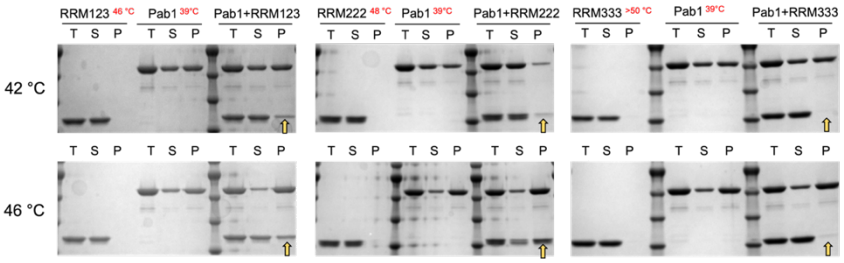

Fig. S11. Co-condensing with Pab1 for RRM123, RRM222 or RRM333 at 42 °C and 46 °C.

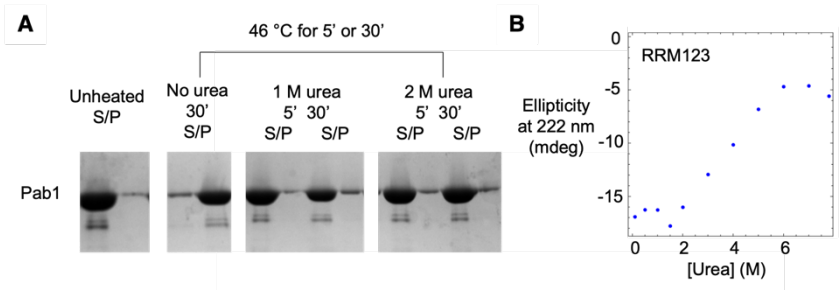

Fig. S12. 1 M urea abolishes Pab1 condensation. (A) Pab1's condensation is inhibited by 1 M urea, analyzed by TSP. The gel lanes are from the same experiment where samples were loaded onto two gels which were treated in parallel. **(B)** Circular dichroism of RRM123 indicates no loss of secondary structure with 1 M urea. Ellipticity at 222 nm is plotted.

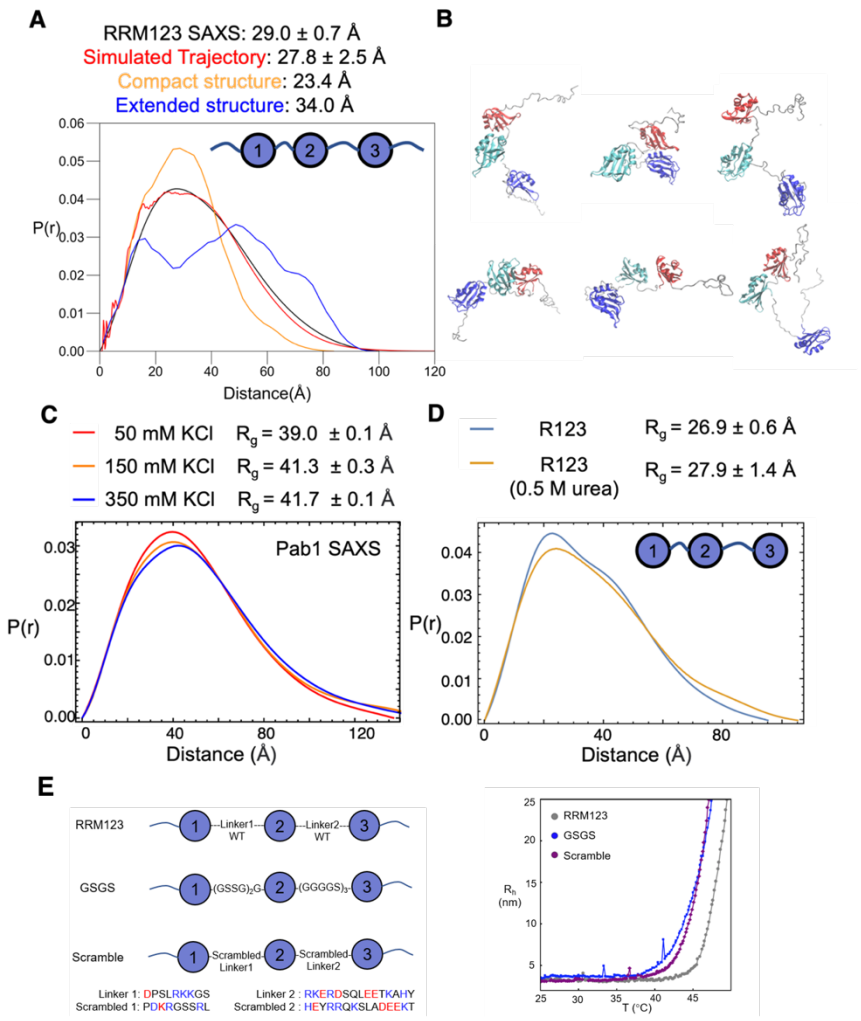

Fig. S13. SAXS studies find that the RRMs are not in a compact, auto-inhibited conformational ensemble prior to condensation. (A) The experimental P(r) for the RRM123 construct having the three amino-terminal RRM domains, is very similar to a P(r) for a simulated conformational ensemble having folded but self-avoiding, non-interacting RRM domains connected by flexible linkers. The provided error in the simulated R_g reflects the variability within the ensemble rather than a calculation error. **(B)** Snapshots of the simulated trajectory. **(C)** The P(r) for Pab1 at three salt concentrations are similar, consistent with the four charged RRM domains being largely non-interacting prior to condensation. **(D)** The P(r) for the R123 construct (RRM1-RRM3 but lacking the flanking disordered regions) is nearly unchanged upon the addition of 0.5 M urea, further supporting a model where the RRMs already are largely non-interacting in the monomeric form without denaturant. **(E)** Linker mutants suggest an inhibitive role of native linkers in condensation. Left: Linker1 (RRM1-RRM2 linker) and linker2 (RRM2-RRM3 linker) are replaced with either GS linker or scrambled sequence linker with the same length while N-termini and linker3 (RRM2-RRM3 linker) are kept the same as WT RRM123. Sequences of scrambled linkers are shown where charged residues are colored (blue for positive, red for negative). Right: DLS of RRM123 WT, GSSG and Scramble mutants, where linker mutants exhibited an earlier T_{cond}.

Table S1: Biochemical and statistical details for HDX

Dataset	Dataset 1			Dataset 2 (data from "Test *Sequential Activation*" session and Fig. S7)[1]			
	Monomeric/soluble (prepared at pH 6.8)	46 °C condensates (prepared at pH 6.8)	pH condensates (prepared at pH 6.5)	Monomeric /soluble (prepared at pH 6.5)	39 °C condensates (prepared at pH 6.5)	42 °C condensates (prepared at pH 6.5)	46 °C condensates (prepared at pH 6.5)
HDX reaction details	50 mM sodium phosphate, 100 mM NaCl, pD_{read} 5.60, on ice	50 mM sodium phosphate, 100 mM NaCl, pD_{read} 5.60, on ice	50 mM sodium phosphate, 100 mM NaCl, pD_{read} 5.60, on ice	50 mM sodium phosphate, 100 mM NaCl, pD_{read} 5.60, on ice	50 mM sodium phosphate, 100 mM NaCl, pD_{read} 5.60, on ice	50 mM sodium phosphate, 100 mM NaCl, pD_{read} 5.60, on ice	50 mM sodium phosphate, 100 mM NaCl, pD_{read} 5.60, on ice
HDX time course (timepoints in parentheses have only 1 bio-replicate)	30 s, (60 s), 100 s, (180 s), 400 s, (600 s), 800 s, (850 s), 1,500 s, (2700 s), 6,000 s, (9,000 s), (13,000 s), 24,000 s	(30 s), 100 s, (200 s), 400 s, (800 s), 1,500 s, 6,000 s, (12,000 s), 22080 s	(10 s), (30 s), 100 s, (200 s), 400 s, 1,500 s, 6,000 s, (12,000 s), 24400 s	100 s, 400 s, 800 s, (1,500 s), 3,000 s, 12,900 s	100 s, 400 s, 800 s, (1,500 s), 3,000 s, 12,000 s	100 s, 400 s, 800 s, 3,000 s, 12,900 s	100 s, 400 s, 800 s, (1,500 s), 3,000 s, 12,900 s
HDX controls	Non-deuterated control, maximally labelled control (50 mM sodium phosphate, 100 mM NaCl, pD_{read} 7.60, 4 °C, overnight)						
Back-exchange (mean; IQR)	27.3%; 14.3%			45.6%; 13.9%			
Number of Peptides	316			273			
Sequence coverage	99%			99%			
Average peptide length/redundancy	12.7/7.1			11.3/5.4			
Replicates	2 bio-replicates						
Repeatability (Root mean square of the paired difference between 2 replicates)	0.69 Da (#D) /5.8% (%D)	0.93 Da (#D) /8.7 % (%D)	0.75 Da (#D) /6.6% (%D)	0.71 Da (#D)/10.3% (%D)	0.71 Da (#D)/10.1% (%D)	0.51 Da (#D) /9.3% (%D)	0.60 Da (#D) /10.2%(%D)
Significant differences in HDX	Rather than compare the difference between states, we compared the k_{obs} to k_{chem} to measure if the region was folded/unstructured, which was clearly discernable in our data.						

[1] The dataset 2 (monomer and 39/42/46 °C condensates prepared at pH 6.5) was collected 1 year after the first dataset collection, during which the experiment apparatus underwent certain modifications.

SI References

1. S. W. Englander, L. Mayne, Y. Bai, T. R. Sosnick, Hydrogen exchange: the modern legacy of Linderstrøm-Lang. *Protein Sci.* **6**, 1101–1109 (1997).

2. G. Kozlov, *et al.*, Solution Structure of the Orphan PABC Domain from Saccharomyces cerevisiae Poly(A)-binding Protein. *Journal of Biological Chemistry* **277**, 22822–22828 (2002).

3. J. A. Riback, *et al.*, Stress-Triggered Phase Separation Is an Adaptive, Evolutionarily Tuned Response. *Cell* **168**, 1028-1040.e19 (2017).

4. A. Bremer, *et al.*, Deciphering how naturally occurring sequence features impact the phase behaviours of disordered prion-like domains. *Nat. Chem.* **14**, 196–207 (2022).